Molecular BioSystems

RSC Publishing

PAPER

View Article Online
View Journal | View Issue

Cite this: *Mol. BioSyst.*, 2013, **9**, 1220

Differential protein profiling of renal cell carcinoma urinary exosomes†

F. Raimondo,‡[a] L. Morosi,‡[a] S. Corbetta,[a] C. Chinello,[a] P. Brambilla,[a] P. Della Mina,[ab] A. Villa,[ab] G. Albo,[c] C. Battaglia,[d] S. Bosari,[e] F. Magni[a] and M. Pitto*[a]

Received 17th December 2012,
Accepted 27th February 2013

DOI: 10.1039/c3mb25582d

www.rsc.org/molecularbiosystems

Renal cell carcinoma (RCC) accounts for about 3% of all human malignancies and its incidence is increasing. There are no standard biomarkers currently used in the clinical management of patients with renal cell carcinoma. A promising strategy for new biomarker detection is comparative proteomics of urinary exosomes (UE), nanovesicles released by every epithelial cell facing the urinary space, enriched in renal proteins and excluding high-abundance plasmatic proteins, such as albumin. Aim of the work is to establish the protein profile of exosomes isolated from urines of RCC patient compared with control subjects. We enrolled 29 clear cell RCC patients and 23 control healthy subjects (CTRL), age and sex-matched, for urine collection and vesicle isolation by differential centrifugation. Such vesicles were morphologically and biochemically characterized and proved to share exosome properties. Proteomic analysis, performed on 9 urinary exosome (UE) pooled samples by gel based digestion followed by LC-MS/MS, led to the identification of 261 proteins from CTRL subject UE and 186 from RCC patient UE, and demonstrated that most of the identified proteins are membrane associated or cytoplasmic. Moreover, about a half of identified proteins are not shared between RCC and control UE. Starting from these observations, and from the literature, we selected a panel of 10 proteins, whose UE differential content was subjected to immunoblotting validation. Results show for the first time that RCC UE protein content is substantially and reproducibly different from control UE, and that these differences may provide clues for new RCC biomarker discovery.

Introduction

Renal cell carcinoma (RCC), a human kidney cancer arising from the proximal tubular epithelium, accounts for 2–3% of all malignancies and is responsible for about 2% of all cancer deaths in Western countries. Among RCC, the clear-cell type displays higher frequency. Since small localized tumors rarely produce symptoms, the diagnosis of RCC is often delayed until the disease is advanced. Moreover, RCC is associated with a high potential of metastasis and is resistant to both chemotherapy and radiotherapy, and nephrectomy remains the most effective treatment.[1–3] Molecularly targeted therapeutic options, mainly addressing products of the VHL pathway, have recently been proven to provide clinical benefits in phase III randomized clinical trials.[4] Accordingly, many RCC biomarker studies have selected components of the VHL pathway for analysis, but despite these promising advances, treatment decisions in RCC still depend on exclusively clinical criteria and there are no standard biomarkers detectable in any biological fluid currently used in the clinical management of patients with renal cell carcinoma.[5,6]

Urine is an ideal biological sample for diagnosis of urologic diseases, because of the ease and noninvasive nature of collection. Moreover, it contains proteins of renal origin and may represent the pathophysiological state of the kidney and the urologic tract.[7] However, many abundant protein species found inside the urinary proteome derive from plasma glomerular filtration. Urinary biomarkers can be obtained from different protein sources, including soluble proteins, sediment proteins, and particle-bound proteins, such as exosomes and microparticles.[8]

[a] *Department of Health Sciences, Univ. of Milano-Bicocca, Via Cadore 48, 20900 Monza, Italy. E-mail: marina.pitto@unimib.it*
[b] *Microscopy and Image Analysis Consortium, University of Milano-Bicocca, Monza, Italy*
[c] *Urology O. U., Fondazione IRCCS Cà Granda, Ospedale Maggiore Policlinico, Milan, Italy*
[d] *Department of Medical Biotechnologies and Translational Medicine, Univ. of Milan, Italy*
[e] *Department of Clinical/Surgical Pathophysiology and Organ Transplant, University of Milan, Fondazione IRCCS Cà Granda, Ospedale Maggiore Policlinico, Milan, Italy*

† Electronic supplementary information (ESI) available. See DOI: 10.1039/c3mb25582d

‡ Equally contributing authors.

Urinary exosomes are 30–100 nm vesicles coated with lipid bilayer membranes, derived from all types of kidney cells that contact the urinary space, including renal tubule cells. Exosomes originate in multivesicular bodies (MVBs) and are secreted into the extracellular fluid through fusion of MVBs with the plasma membrane.[9–11] The use of urinary exosomes as a starting material for biomarker discovery was shown to be advantageous, since reduction of the complexity of the urine proteome together with enrichment in renal proteins towards the plasmatic ones is achieved.[12] In fact, exosome protein content accounts for about 3% of the total proteins in normal urine, and it is depleted from the most abundant ones, such as albumin.[13] Moreover, since exosomes from different cell types have different components, it is likely that the exosome proteome could better reflect, with respect to native urine, the cellular processes associated with the pathogenesis of RCC. In fact, it was suggested that urinary exosome excretion may play a role in regulating renal epithelial protein content.[14]

Accordingly, several proteomic studies on urinary exosomes have been performed to identify biomarkers predictive of urinary track diseases, both in experimental and clinical settings.[7,13,15–18] For an exhaustive review see Moon *et al.*[19] However no proteomic study of urinary exosomes has been yet accomplished in RCC.

Therefore, we performed MS profiling and antibody-based validation and quantification of differential proteins in urinary exosomes from a RCC patient cohort in order to search for a potential tumor marker.

Material and methods

Chemicals

Milli-Q water was used for all solutions. BCA protein assay, trifluoroacetic acid, ammonium bicarbonate, porcine trypsin DTT, iodoacetamide, Trizma-base, ACN, methanol, and CAPS were from SIGMA Chemical Co. (St. Louis, MO, USA); glycerol was from Merck (Darmstadt, Germany). Paraformaldehyde, osmium tetroxide (OsO_4), cacodylate buffer and LRW resin were from Electron Microscopy Sciences (Hatfield, PA, USA). The Hybond-ECL nitrocellulose membrane was from GE (Little Chalfont, Buckinghamshire, UK). NuPAGE® SDS-PAGE Gel Electrophoresis System components (mini gels, running and loading buffers, molecular weight markers and Coomassie blue staining) were supplied by Life Technologies (Paisley, Renfrewshire, UK). An anti-protease inhibitor cocktail (Complete) was from Roche (Monza, Italy). OptiPrepTM solution was from Axis-Shield (Oslo, Norway). The monoclonal anti-Flotillin 1 (Flot1) antibody was purchased from Transduction Laboratories (Lexington, KY, USA); the polyclonal anti-Dipeptidase1 (DPEP) antibody from Genetex Inc. (Irvine, CA, USA); the polyclonal anti-extracellular matrix metalloproteinase inducer (EMMPRIN/CD147/Basigin) antibody from Zymed (San Francisco, USA); the polyclonal anti-syntenin 1 (SDCBP) antibody from Abnova (Taipei, Taiwan); the monoclonal anti-Aquaporin1 (AQP1) antibody from Santa Cruz Biotechnology (Santa Cruz, CA, USA); monoclonal anti-tumor susceptibility gene 101 (TSG10), anti-motility-related protein 1 (CD9), polyclonal anti-podocalixyn (PODXL) and anti-neprilysin (CD10) antibodies from Abcam (Cambridge, UK); polyclonal anti-dickkopf related protein 4 (DKK4) from Abgent (San Diego, CA, USA); monoclonal anti-matrix metalloproteinase-9 (MMP9) from BD Bioscience (San José, CA, USA); monoclonal anti-carbonic anhydrase IX (CAIX) is a kind gift from Dr Silvia Pastorekova (Slovak Academy of Sciences, Bratislava, Slovak Republic). Species-specific secondary peroxidase conjugated antibodies and ECL reagents were from Pierce (Rockford, IL, USA).

Collection of human urine and normalization

Second morning urine samples (about 50 mL) were collected, according to EuroKUP guidelines (http:www.eurokup.org) and after the informed consent was approved by the Local Research Ethics Committee, from 29 RCC patients (age 40–86, mean 63.5, 19 males and 10 females) before surgery, and 23 healthy control subjects, matched for sex and age (age 50–78, mean, 59.2, 13 males and 10 females), and stored at −80 °C. The study protocol, informed consent and procedures were approved by the Local Research Ethics Committee of IRCCS Cà Granda, Ospedale Maggiore Policlinico and were in agreement with the Declaration of Helsinki.

A brief description of the patients involved in this study is shown in Table 1, and more detailed in Table S1 in ESI.† None of the patients had received previous chemotherapy. RCC was classified according to WHO recommendations[20] also using immunohistochemical techniques: only samples from diagnosed conventional clear cell RCC (ccRCC) were included in the study. Tumour staging and grading were assigned, according to the 2009 TNM (Tumor, Node, Metastasis) system classification, by a pathologist.

An aliquot of the collected urine samples was subjected to routine chemical–physical examination. Moreover, creatinine assay (Jaffé method, Roche) was performed on individual urine samples to normalize the gel loading of proteins to account for differences in urine concentration.[21]

Purification of exosomes

Exosomes were prepared from each patient's urine sample by differential centrifugation[22] and according to guidelines provided by EuroKUP (http:www.eurokup.org). Briefly, after sediment removal (10 min at 1000 × *g*, 4 °C) and addition of protease inhibitors (Complete, Roche), urine samples were

Table 1 Clinical characteristics of enrolled ccRCC patients

G	pT	Number of patients
1	2a	1
	1a	5
2	1b	10
	2a	6
2–3	1b	1
	1a	1
	1b	3
3	2a	1
	2b	1

centrifuged for 15 min at 17 000 × *g* and 4 °C, to eliminate large membrane fragments and debris. Supernatants were subjected to ultracentrifugation for 1 h at 200 000 × *g* and 4 °C: crude exosome pellets were washed in PBS and then resuspended in bidistilled water, in the presence of protease inhibitors. The samples were stored at −80 °C until use.

In some cases, in order to verify the efficacy of further purification, the crude exosomes were subjected to Optiprep™ density gradient ultracentrifugation.[23] Briefly, the crude exosome pellet was overlaid on a discontinuous OptiPrep gradient (40, 20, 10, and 5% OptiPrep solution in 0.25 M sucrose, 10 mM Tris, pH 7.5) and centrifuged at 100 000 × *g* for 16 h. Twelve fractions (1 mL) were collected from the top of the gradient, diluted with 2 mL of 10 mM Tris buffer, and centrifuged at 100 000 × *g* for 3 h; after washing with PBS, the obtained pellets were subjected to further analysis. The density of each fraction was determined by absorbance at 244 nm using a duplicate parallel discontinuous OptiPrep gradient overlaid with 500 μL of 0.25 M sucrose, 10 mM Tris, pH 7.5.[24]

Moreover, we analyzed the protein composition of urine samples after sediment removal (U), and of the supernatants after 200 000 × *g* ultracentrifugation (Sn).

In order to concentrate proteins, urine and Sn samples were subjected to ultrafiltration: briefly, 500 μL of urine samples were loaded onto concentrator devices, VivaSpin 500 (3000 MW cut-off PES membrane, Sartorius), pre-treated with 5% Triton-X100 for improved recovery of low-concentrated samples, according to the manufacturer's instruction. After a 45 min centrifugation at 15 000 × *g* (4 °C), the concentrate was collected and lyophilized.

Protein concentration was assessed by BCA assay (Sigma).

For protein identification and deglycosylation experiments, representative UE derived from 9 RCC and 9 CTRL urine samples were pooled and proteins separated by 4–12% gel electrophoresis, followed by LC-MS/MS analysis.

Transmission electron microscopy

In order to validate exosome purity, Transmission Electron Microscopy (TEM) imaging of exosomes was performed as below. Briefly, after exosome purification, fresh exosomal preparations were fixed with 4% paraformaldehyde and deposited on Formvar-carbon-coated Nickel grids. Samples were post-fixed in 1% OsO4 in cacodylate buffer, dehydrated in ethanol and embedded in LRW resin. Grids were doubly stained with uranyl acetate and lead citrate and examined using a transmission electron microscope CM 10 Philips (FEI, Eindhoven, the Netherlands).

Deglycosylation of exosome proteins

Removal of N- and O-linked glycans was performed using the Glycoprotein Deglycosylation kit (Merck, Nottingham, UK) according to the manufacturer's instructions.[25] Briefly, proteins (15 μg) from pooled RCC and CTRL exosomes were dissolved in reaction buffer (50 mM sodium phosphate buffer, pH 7.0) in the presence of anti-proteases. Proteins were incubated with denaturing solution (0.2% w/v SDS, 100 mM β-mercaptoethanol), at 100 °C for 5 minutes; then, Triton X-100 (0.75%) was added to complex any free SDS. Enzymatic deglycosylation was carried out by the addition of 1 μL of PNGase F (5000 U mL^{-1}), 1 μL of *endo*-α-*N*-acetylgalactosaminidase (1.25 U mL^{-1}), 1 μL of α-2–3,6,8,9-neuraminidase (5.0 U mL^{-1}), 1 μL of β-*N*-acetylglucosaminidase (45 U mL^{-1}), and 1 μL of β-1,4-galactosidase (3.0 U mL^{-1}), and samples were incubated overnight at 37 °C. Bovine fetuin was deglycosylated under the same conditions, and used as a control.

Electrophoresis and western blotting

Equal amounts of exosome, urine and Sn proteins were separated by 4–12% NuPAGE (Life technologies) and transferred to nitrocellulose membranes, using a mini transfer tank (Hoefer). After blocking with 5% free-fat milk/0.2% Tween 20 in PBS solution, the blots were developed with the respective primary antibodies followed by a peroxidase-conjugated secondary antibody (Pierce) and enhanced chemiluminescence detection (SuperSignal West-Dura ECL, Pierce) by a CCD camera (Kodak ds Image Station 2000 R). Densitometric analysis was performed by molecular Imaging Software (Kodak) and the volumes of band proteins were normalized to urinary creatinine content.[14] Evaluation of diagnostic performance was accomplished by ROC analysis (GraphPad Prism 5, GraphPad Software, Inc.).

For mass spectrometry analysis, pooled exosome proteins were separated using a 4–12% NuPAGE electrophoresis system (Life Technologies), and subjected to Coomassie Blue staining.

Mass spectrometry and protein identification

The bands of interest were excised from gels and subjected to in-gel protein digestion as already described by Raimondo *et al.*[26] Briefly, the gel plugs were washed twice with a mixture of 25 mM NH_4HCO_3–ACN (1 : 1; v/v) for 15 min. After 45 minute reduction at 56 °C with 10 mM DTT, protein bands were alkylated with 55 mM of IAA (dark; 30 min). Gel slices were then washed again using ammonium bicarbonate, 25 mM, with 50% acetonitrile for three times. After dehydration with acetonitrile, the proteins were in-gel digested with modified porcine trypsin (Promega, Madison, WI, USA; 12.5 ng μL^{-1} in 25 mM NH_4HCO_3) at 37 °C overnight (8 μL for each sample). Digested peptide solutions were then diluted in TFA 0.1% and the entire volume was injected into nLC ESI MS/MS.

Protein identification was performed on a Proxeon EasynLC System (Proxeon Biosystems, Odense, Denmark) coupled with a MaXis hybrid UHR-QToF system (Bruker Daltonics, Bremen, DE). After injection, trypsinized samples were thus desalted onto a 2 cm precolumn (ID 100 μm, 5 μm, C18–A1, EasycolumnTM, Proxeon) and separated with a flow of 300 nL min^{-1} on a 10 cm fused silica micro-capillary analytical column (ID 75 μm, 3 μm, C18–A2, EasycolumnTM, Proxeon) using a 60 min gradient from 2 to 56% of acetonitrile containing 0.1% of formic acid in 25 min and then from 56 to 98% in 10 min. The EasynLC column was directly connected to the ESI source with a nanosprayer system (Bruker Daltonics, Bremen, DE). MS level measurements were all performed on a predefined 50–2200 *m*/*z* acquisition window at 1 Hz spectra rate. To improve mass accuracy a specific lock mass (1221.9906 *m*/*z*) was used. CID MS/MS acquisition was performed over a 400–1600 *m*/*z* window (excluding 1221.5–1224 *m*/*z*) with five intensity binned

precursors of preferred charge state range +2 to +4, with at least 2000 counts selected for fragmentation. Selected precursors that had been analysed more than once were actively excluded from analysis for 30 s. Isolation width and collision energy were applied on the basis of isolation mass value and charge state against a table of isolation and fragmentation lists fitted for tryptic peptides. The total cycle time ranged from 6 to 11 seconds. Ion transmission for MS–MS was also performed by setting key parameters for the collision cell and the ion cooler cell as follows: CCRF = 1200 Vpp and ICRF = 400 Vpp; transfer time ICTT = 100 μs and pre-pulse time ICPP = 8 μs.

Raw MS/MS data were lock-mass corrected, deconvoluted and converted to an XML peaklist *via* Compass DataAnalysis v.4.0 Sp4 (BrukerDaltonics). Peakfinder (sumpeaks) was set to exclude any ions with $S/N < 1$ and intensity <20 counts. In house Mascot search engine (Version: 2.3.02) was used for processing XML data. Database searching was restricted to the human Swissprot (accessed Feb 2012; 20,317 sequences) database. Searches were performed against the database using the following parameters: fully tryptic enzymatic cleavage with one possible missed cleavage, a peptide tolerance of 10 ppm, and a fragment ion tolerance of 0.5 Da. Fixed modification was set as carbamidomethyl due to carboxyamidomethylation of cysteine residues. Mascot threshold scores for identity were used as peptide level filters of peptide significance. Protein identifications with a Mascot score above the significant hit threshold ($p < 0.05$) and at least one identical peptide were considered significant.

Results and discussion

Urinary vesicle isolation and characterization

Urine samples were collected from 29 RCC patients and 23 healthy controls, matched for sex and age. The patients display quite homogeneous clinical features, most of them were in early phases of disease, with no metastasis nor positive lymph nodes at the moment of diagnosis (Table 1; Tables S1 and S2 in ESI†).

All the patient and control subject urine samples were negative for proteins, glucose, ketone, bilirubin, urobilinogen, and blood.

After urinary vesicle isolation, their protein concentration was assessed, and referred to the initial urine volume (Tables S1 and S2 in ESI†). It is highly variable, as already reported, ranging from 0.99 to 16 μg mL^{-1} of starting urine samples in patients, and from 2.78 to 11.8 μg mL^{-1} in controls.[27]

In order to validate the exosome purification protocol, we performed western blot analysis on the ultracentrifugation pellets, in comparison with starting urine samples and the ultracentrifugation supernatants (after suitable protein concentration), using antibodies against three commonly used urinary exosomal markers, CD9, TSG101 and Flotillin-1.[28] Results show that urinary exosome-associated protein signals were predominant in the vesicle fraction, and nearly undetectable in total urine or the supernatant (Fig. 1A). Therefore markers are highly and reproducibly enriched in the vesicle fraction, both in RCC and in controls (Fig. 1B).

It has been reported[29] that efficient isolation and purification of urinary exosomes facilitate quantitative and reproducible proteomic investigation. However, this is obtained at the expense of a very low recovery, and leads to the requirement of huge amounts of starting material (as much as 1 L of urine samples). This seems quite unsuited with the clinical needs. Indeed, our results obtained by the application of a more stringent isolation method (Optiprep gradient) show that exosome markers are mainly detectable in fraction 7, at a density of 1.10 g mL^{-1}, as reported.[30] However, it did not lead to a substantially increased enrichment (Fig. S1 in the ESI†), compared with an ultracentrifugation protocol (CE, crude exosomes), while the yield was much lower.

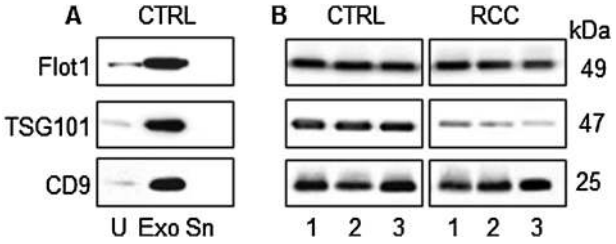

Fig. 1 Urinary exosome protein markers. (A) Immunoblotting for known exosomal markers (CD9, TSG101 and Flot1) in vesicle fraction (Exo), in comparison with total urine sample after sediment removal (U), and with the supernatant (Sn), obtained after 200 000 × *g* ultracentrifugation from a representative control subject (CTRL). (B) Immunoblotting for the same markers in exosomal samples from 3 representative CTRL subjects and RCC patients. Equal amounts of proteins were loaded on all the lanes of each gel.

Moreover, UE morphology, shape and dimension were examined by electron microscopy, followed by morphometric analysis. Vesicles are shown to have spherical shape and mean diameter comprised between 30 and 50 nm, indicating that the population of vesicles, prepared by UC, which we are dealing with, is constituted mainly of real exosomes; in fact, the spherical shape and the mean dimensions (Fig. 2 and 3) agree with data present in the literature.[30] Moreover, there are no important morphological differences between exosomes in the two groups (patients and controls), as shown also by the morphometric analysis (Fig. 2A, B and 3).

Also in this case, when we further purified vesicles by the Optiprep gradient, we did not observe any substantial change in the vesicle appearance, except for the presence of a cleaner background (Fig. S2 in the ESI†), confirming data regarding marker enrichment. Accordingly, we concluded that the crude preparations contain ''bona fide'' exosomes.

Electrophoresis analysis

In this study, the molecular weight distribution of UE proteins was observed by NuPAGE, followed by Coomassie Blue staining. As shown in Fig. 4, the distribution of protein bands following gel electrophoresis was similar in starting urine and in the supernatant after centrifugation at 200 000 × *g*; instead, the distribution of protein bands was different in UE samples, determining a typical protein profile: in fact albumin, responsible for the main band appearance in the non-exosomal fractions, results depleted, while THP, a glycoprotein released by kidney tubular cells, is predominant in the UE profile,

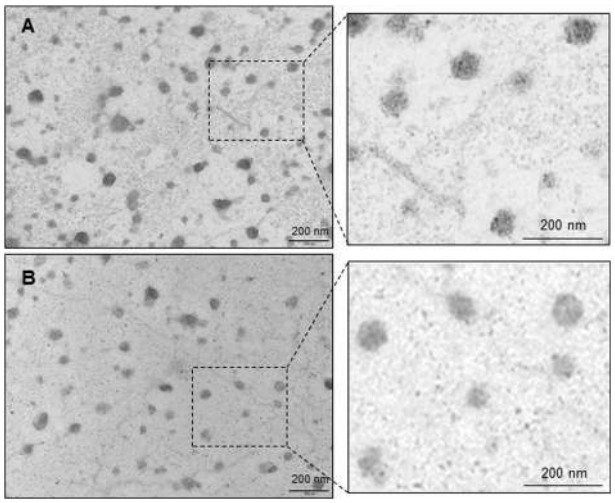

Fig. 2 Morphological characterization of urinary exosomes. Electron micrographs of crude exosomes doubly stained with uranyl acetate and lead citrate, and examined by transmission electron microscope CM 10 Philips: (A) control UE; (B) RCC UE.

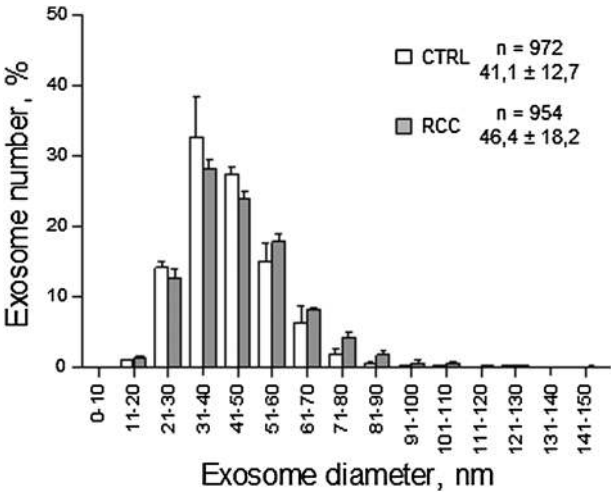

Fig. 3 Size distribution (mean ± SD) of urinary exosomes. A total of 15 fields from two control subjects and two RCC patients were analyzed.

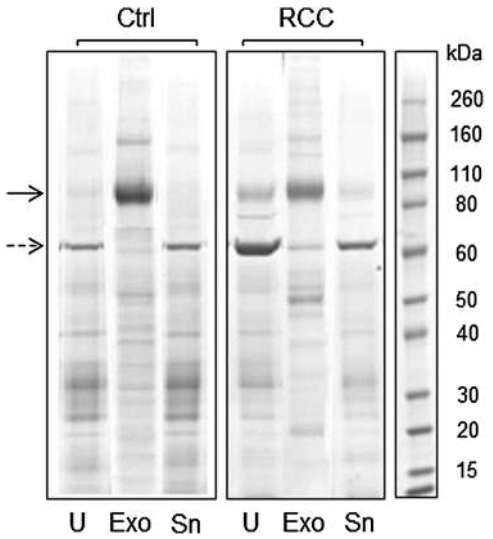

Fig. 4 Protein profiles by NuPAGE 4–12% of vesicle fraction (Exo), compared with total urine samples after sediment removal (U), and with supernatant (Sn), obtained after 200 000 × *g* ultracentrifugation, from one representative control subject (CTRL) and one RCC patient. Solid and dashed arrows indicate the position of THP and albumin, respectively, both identified by MS (see ESI,† Tables S3 and S4).

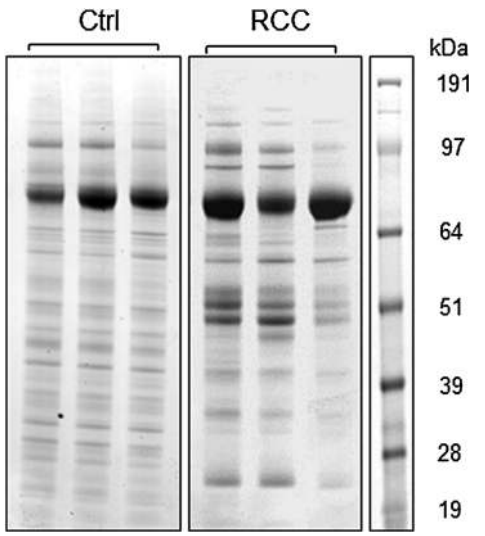

Fig. 5 Protein profiles by NuPAGE 4–12% of vesicle fraction (Exo), isolated from urine samples of three representative control subjects and RCC patients.

although with different intensity in the different lanes (see also Fig. 5). The variable content of THP may also explain the variations encountered in total protein UE recovery (see above).

Moreover, apart from THP, the exosomal protein composition was similar inside the same group (of RCC patients and healthy controls), while it showed evident differences between these two groups (Fig. 5). We also checked that the stability of the similarity and the reproducibility of the differences were independent of the time of collection (data not shown). Therefore a consistent reproducibility is assured (Fig. 5).

Relying on this observation, we selected some representative UE samples for pooling, aimed at proteomic analysis, before and after enzymatic deglycosylation. Deglycosylation determined substantial changes in the UE protein profile, with an evident shift of THP glycoprotein bands towards lower molecular weights (Fig. S3 in ESI†).

Protein identification

In order to investigate the RCC and healthy control UE protein profiles, we prepared a pool of UE from 9 different patients and another one from 9 healthy subjects. This allowed us to have enough material and to reduce the effect of interpersonal variability. We identified 261 proteins in CTRL subjects' UE and 186 in RCC patients' UE, some of which only after deglycosilation, likely due to the uncovering of some bands and the

Table 2 List of proteins identified only in urinary exosomes isolated from control subject urine samples

Name	Accession (UNIPROT)	MW (Da)	Mascot score	Localization
Metabolic enzymes				
1,5-Anhydro-D-fructose reductase	Q96JD6	37 136	21	Cytoplasm
15-Hydroxyprostaglandin dehydrogenase [NAD+]	P15428	29 187	59	Cytoplasm
3-Hydroxybutyrate dehydrogenase type 2	Q9BUT1	27 049	51	Cytoplasm
Alcohol dehydrogenase [NADP+]	P14550	36 892	21	Other/unknown
Calpain-7	Q9Y6W3	93 335	40	Other/unknown
Carboxymethylenebutenolidase homolog	Q96DG6	28 372	24	Cytoplasm
Dihydropteridine reductase	P09417	26 001	31	Cytoplasm
Fidgetin-like protein 1	Q6PIW4	74 829	24	Other/unknown
Fructose-1,6-bisphosphatase 1	P09467	37 218	31	Cytoplasm
γ-Butyrobetaine dioxygenase	O75936	45 200	32	Cytoplasm
Glucose-6-phosphate isomerase	P06744	63 335	36	Cytoplasm
Glutathione S-transferase A2	P09210	25 648	74	Cytoplasm
Glutathione S-transferase ω-1	P78417	27 833	33	Cytoplasm
Glutathione S-transferase P	P09211	23 569	32	Other/unknown
Glycerol-3-phosphate dehydrogenase [NAD+]	P21695	38 171	27	Cytoplasm
Histone H2A type 1-A	Q96QV6	45 087	82	Organelles
Maltase-glucoamylase	O43451	211 031	94	Plasmamembrane
Non-secretory ribonuclease	P10153	18 855	37	Organelles
Peroxiredoxin-1	Q06830	22 324	35	Cytoplasm
Protein S100-A6	P06703	59 899	97	Organelles
Pyruvate kinase isozymes M1/M2	P14618	58 470	60	Cytoplasm
Ribonuclease inhibitor	P13489	51 766	28	Cytoplasm
Triosephosphate isomerase	P60174	26 938	111	Other/unknown
Ubiquitin-conjugating enzyme E2 variant 3	Q8IX04	52 516	29	Other/unknown
Xaa-Pro dipeptidase	P12955	55 311	25	Plasmamembrane
Signalling				
14-3-3 Protein ε	P31946	29 326	56	Cytoplasm
14-3-3 Protein z/δ	P63104	27 899	74	Cytoplasm
ADP-ribosyl cyclase 2	Q10588	36 328	44	Plasmamembrane
Annexin A4	P09525	36 088	340	Cytoplasm
Calbindin	P05937	30 291	46	Cytoplasm
Cofilin-1	P23528	18 719	45	Cytoplasm
G-protein coupled receptor family C group 5 member B	Q9NZH0	45 279	140	Plasmamembrane
G-protein coupled receptor family C group 5 member C	Q9NQ84	48 732	103	Plasmamembrane
G-protein G(I) subunit α-2	P04899	40 995	86	Plasmamembrane
G-protein G(I)/G(S)/G(T) subunit β-2	P62879	38 048	69	Plasmamembrane
G-protein subunit α-13	Q14344	44 364	48	Plasmamembrane
Neprilysin	P08473	86 144	151	Plasmamembrane
Programmed cell death protein 10	Q9BUL8	24 686	34	Plasmamembrane
Proto-oncogene tyrosine-protein kinase Src	P12931	60 310	33	Plasmamembrane
Ras-related C3 botulinum toxin substrate 2	P15153	21 814	36	Cytoplasm
Ras-related protein Ral-B	P11234	23 508	53	Plasmamembrane
Ras-related protein Rap-1A	P62834	21 316	63	Plasmamembrane
Ras-related protein R-Ras2	P62070	23 613	42	Plasmamembrane
Rho guanine nucleotide exchange factor 10-like protein	Q9HCE6	141 873	26	Cytoplasm
Tetraspanin-1	O60635	26 910	68	Plasmamembrane
Transforming protein RhoA	P61586	22 096	26	Plasmamembrane
Vesicular trafficking				
14 225	Q9H1C7	11 488	36	Plasmamembrane
ADP-ribosylation factor 6	P62330	20 183	62	Organelles
Annexin A1	P04083	38 918	105	Plasmamembrane
Annexin A7	P20073	52 991	108	Secreted
Charged multivesicular body protein 1b	Q7LBR1	22 152	112	Organelles
Charged multivesicular body protein 2a	O43633	25 088	81	Organelles
Charged multivesicular body protein 4b	Q9H444	24 935	148	Organelles
Charged multivesicular body protein 5	Q9NZZ3	24 612	51	Organelles
Copine-3	O75131	60 947	68	Cytoplasm
Copine-8	Q86YQ8	63 638	34	Other/unknown
EH domain-containing protein 1	Q9H4M9	60 646	84	Plasmamembrane
EH domain-containing protein 4	Q9H223	61 365	107	Plasmamembrane
Lysosome-associated membrane glycoprotein 1	P11279	45 367	75	Organelles
Multivesicular body subunit 12A	Q96EY5	29 107	56	Organelles
Ras-related protein Rab-10	P61026	22 755	92	Plasmamembrane
Ras-related protein Rab-11A	P62491	24 492	71	Plasmamembrane
Ras-related protein Rab-11B	Q15907	24 588	53	Plasmamembrane
Ras-related protein Rab-2A	P61019	23 702	36	Organelles
Ras-related protein Rab-3A	P20336	25 196	53	Plasmamembrane

Table 2 (*continued*)

Name	Accession (UNIPROT)	MW (Da)	Mascot score	Localization
Ras-related protein Rab-5B	P61020	23 920	47	Plasmamembrane
Ras-related protein Rab-8B	Q92930	23 740	45	Plasmamembrane
Vacuolar protein sorting-associated protein 28	Q9UK41	25 694	65	Plasmamembrane
Vacuolar protein sorting-associated protein 37D	Q86XT2	27 941	82	Organelles
Vacuolar protein sorting-associated protein 4A	Q9UN37	49 152	77	Organelles
Vacuolar protein sorting-associated protein VTA1 homolog	Q9NP79	34 143	39	Organelles
WASH complex subunit strumpellin	Q12768	135 113	34	Organelles
Transport				
Aquaporin-2	P41181	29 047	45	Plasmamembrane
Chloride intracellular channel protein 4	Q9Y696	28 982	31	Plasmamembrane
Cytochrome b reductase 1	Q53TN4	31 735	32	Plasmamembrane
Electrogenic sodium bicarbonate cotransporter 1	Q9Y6R1	122 295	25	Plasmamembrane
MIT domain-containing protein 1	Q8WV92	29 638	67	Organelles
Multidrug resistance protein 1	P08183	141 788	65	Plasmamembrane
Na(+)/H(+) exchange regulatory cofactor NHE-RF3	Q5T2W1	57 379	21	Plasmamembrane
Protein MAL2	Q969L2	19 341	51	Plasmamembrane
Proton-coupled amino acid transporter 2	Q495M3	53 809	37	Plasmamembrane
Ras-related protein Rab-1A	P62820	22 891	78	Organelles
Retinol-binding protein 5	P82980	16 092	39	Cytoplasm
Selenium-binding protein 1	Q13228	52 928	43	Cytoplasm
Solute carrier family 12 member 3	P55017	114 193	70	Plasmamembrane
Solute carrier family 22 member 2	O15244	63 265	30	Plasmamembrane
Solute carrier family 23 member 1	Q9UHI7	65 644	27	Plasmamembrane
V-type proton ATPase subunit B, brain isoform	P21281	56 807	24	Organelles
V-type proton ATPase subunit B, kidney isoform	P15313	57 196	26	Organelles
V-type proton ATPase subunit C 1	P21283	44 085	21	Organelles
Adhesion/cytoskeleton				
Galectin-3	P17931	26 193	27	Cytoplasm
Insulin-like growth factor-binding protein 7	Q16270	30 138	28	Secreted
Actin-related protein 2/3 complex subunit 2	O15144	34 426	37	Cytoskeleton
Annexin A11	P50995	54 697	655	Cytoskeleton
Brain-specific angiogenesis inhibitor 1-associated protein 2	Q9UQB8	61 115	40	Cytoplasm
Desmoplakin	P15924	334 021	29	Cytoskeleton
Kinesin-like protein KIF12	Q96FN5	71 813	29	Cytoskeleton
Macrophage-capping protein	P40121	38 779	32	Cytoplasm
Myosin-1c	O00159	122 503	156	Cytoplasm
Nck-associated protein 1	Q9Y2A7	130 018	48	Organelles
Nesprin-1	Q8NF91	1 017 069	18	Cytoskeleton
Perlecan	P98160	479 221	29	Secreted
Profilin-1	P07737	15 216	30	Cytoskeleton
Putative β-actin-like protein 3	Q9BYX7	42 331	42	Cytoskeleton
Radixin	P35241	68 635	100	Plasmamembrane
Uroplakin-2	O00526	103 846	32	Cytoskeleton
WD repeat-containing protein 1	O75083	66 836	23	Cytoplasm
Immune response				
Thioredoxin	P10599	77 224	116	Secreted
Toll-interacting protein	Q9H0E2	30 490	78	Cytoplasm
Xaa-Pro aminopeptidase 2	O43895	76 090	32	Plasmamembrane
Others/unknowns				
CD2-associated protein	Q9Y5K6	71 635	43	Cytoskeleton
Ankyrin repeat and FYVE domain-containing protein 1	Q9P2R3	129 915	69	Organelles
Annexin A6	P08133	76 168	97	Cytoplasm
Azurocidin	P20160	27 325	26	Cytoplasm
Brain acid soluble protein 1	P80723	22 680	116	Plasmamembrane
Brevican core protein	Q96GW7	100 539	22	Secreted
Centrosomal protein of 290 kDa	O15078	290 892	27	Cytoplasm
Chromobox protein homolog 2	Q14781	56 388	21	Other/unknown
Coiled-coil and C2 domain-containing protein 1A	Q6P1N0	104 397	45	Cytoplasm
Cullin-associated NEDD8-dissociated protein 1	Q86VP6	137 999	36	Other/unknown
DNA excision repair protein ERCC-6	Q03468	169 452	27	Other/unknown
Elongation factor 1-α 1	P68104	50 451	53	Cytoplasm
Heat shock 70 kDa protein 1-like	P34931	70 730	44	Cytoplasm
Histone H3.1t	Q16695	14 225	26	Other/unknown
Histone H4	P62805	10 966	86	Other/unknown
Hsc70-interacting protein	P50502	41 477	72	Cytoplasm
Lysosomal protective protein	P10619	54 944	59	Organelles

Table 2 (*continued*)

Name	Accession (UNIPROT)	MW (Da)	Mascot score	Localization
Myeloperoxidase	P05164	84 784	61	Organelles
PDZK1-interacting protein 1	Q13113	12 333	51	Plasmamembrane
Peflin	Q9UBV8	30 646	46	Cytoplasm
Phosphatidylethanolamine-binding protein 1	P30086	21 158	108	Cytoplasm
Proactivator polypeptide	P07602	11 360	111	Other/unknown
Probable Xaa-Pro aminopeptidase 3	Q9NQH7	57 624	25	Organelles
Prolactin-inducible protein	P12273	16 847	33	Secreted
Protein S100-A9	P06702	13 291	82	Cytoplasm
Semenogelin-1	P04279	52 157	44	Secreted
Semenogelin-2	Q02383	65 519	27	Secreted
THAP domain-containing protein 4	Q8WY91	63 535	23	Other/unknown
Transmembrane protease serine 2	O15393	55 079	39	Plasmamembrane
Transmembrane protein C19orf77	O75264	15 012	53	Plasmamembrane
Tubulin polyglutamylase TTLL7	Q6ZT98	12 015	83	Cytoplasm
Tyrosine-protein kinase FRK	P42685	58 673	35	Cytoplasm
Uroplakin-1a	O00322	29 429	32	Plasmamembrane
Vesicle-associated membrane protein 8	Q9BV40	19 540	83	Plasmamembrane
Vitamin K-dependent protein Z	P22891	46 026	26	Secreted

Mascot score = Mascot threshold scores for identity were used as peptide level filters of peptide significance. Protein identifications with a Mascot score above the significant hit threshold ($p < 0.05$) and at least one identical peptide were considered significant. Localization = subcellular localization based on UniProtKB.

Table 3 List of proteins identified only in urinary exosomes isolated from RCC patient urine samples

Name	Accession (UNIPROT)	MW (Da)	Mascot score	Localization
Metabolic enzymes				
1-Acyl-*sn*-glycerol-3-phosphate acyltransferase α	Q99943	32 038	32	Plasmamembrane
6-Phosphogluconolactonase	O95336	27 815	123	Organelles
Abhydrolase domain-containing protein 14B	Q96IU4	22 446	47	Organelles
Aspartate aminotransferase	P17174	46 447	23	Organelles
Bile salt-activated lipase	P19835	79 614	29	Secreted
Carbonic anhydrase 1	P00915	28 909	21	Organelles
Dipeptidyl peptidase 2	Q9UHL4	54 763	19	Organelles
Lysosomal acid phosphatase	P11117	48 713	115	Organelles
N-Acetylgalactosamine-6-sulfatase	P34059	58 445	26	Organelles
Pepsin A	P00790	42 350	43	Secreted
Peroxiredoxin-2	Q06830	22 049	46	Organelles
Phosphoglycerate kinase 1	P00558	44 985	28	Organelles
Prostate-specific antigen	P07288	29 293	27	Secreted
Tissue α-L-fucosidase	PO4066	53 940	25	Organelles
Signalling				
Angiotensinogen	P01019	53 406	22	Secreted
Chondroitin sulfate proteoglycan 4	Q6UVK1	251 067	95	Plasmamembrane
Dapper homolog 1	Q9NYF0	91 145	31	Cytoplasm
Dickkopf-related protein 4	Q9UBT3	26 057	14	Secreted
G-protein G(S) subunit α isoforms XLas	Q5JWF2		79	Plasmamembrane
Ras-related C3 botulinum toxin substrate 1	P63000	21 835	25	Plasmamembrane
Vasorin	Q6EMK4	72 751	72	Plasmamembrane
Vesicular trafficking				
Ras-related protein Rab-1A	P62820	22 891	66	Organelles
Transport				
Apolipoprotein A-I	P02647	30 759	71	Secreted
Ceruloplasmin	P00450	122 983	274	Secreted
Cytochrome b561	P49447	27 713	24	Plasmamembrane
Hemoglobin subunit β	P68871	16 102	72	Other/unknown
Nuclear transport factor 2	P61970	14 640	34	Cytoplasm
Receptor activity-modifying protein 2	O60895	19 880	21	Plasmamembrane
Serotransferrin	P02787	79 280	349	Secreted
Thyroxine-binding globulin	P05543	46 637	21	Secreted
Transthyretin	P02766	15 991	48	Secreted
Adhesion (cytoskeleton)				
Actin-related protein 2/3 complex subunit 4	P59998	19 768	27	Cytoskeleton
Collagen α-3(VI) chain	P12111	345 167	44	Secreted
F-actin-capping protein subunit α-1	P52907	33 073	51	Cytoplasm

Table 3 (*continued*)

Name	Accession (UNIPROT)	MW (Da)	Mascot score	Localization
Immune response				
Annexin A3	P12429	36 524	35	Secreted
Complement C3	P01024	188 569	231	Secreted
Complement C4-A	P0C0L4	194 247	52	Secreted
Complement component C9	P02748	64 615	32	Plasmamembrane
Endothelial protein C receptor	Q9UNN8	26 997	66	Plasmamembrane
Ig γ-3 chain C region	P01860	42 287	89	Secreted
Ig heavy chain V-III region TIL	P01765	12 462	85	Secreted
Ig heavy chain V-III region VH26	P01764	12 745	54	Secreted
Ig κ chain V-III region SIE	P01620	11 882	100	Secreted
Ig κ chain V-III region VG (Fragment)	P04433	12 681	38	Secreted
Ig κ chain V-IV region (Fragment)	P06312	13 486	49	Secreted
Ig κ chain V-IV region Len	P01625	12 746	39	Secreted
Ig λ chain V-III region LOI	P80748	12 042	33	Secreted
Inter-α-trypsin inhibitor heavy chain H4	Q14624	103 521	132	Secreted
Monocyte differentiation antigen CD14	P08571	40 678	30	Plasmamembrane
Peptidoglycan recognition protein 1	O75594	22 116	73	Secreted
Serpin B3	P29508	44 594	103	Cytoplasm
TIR domain-containing adapter molecule 1	Q8IUC6	77 343	17	Plasmamembrane
α1-Antitrypsin	P01009	46 878	354	Secreted
Others/unknown				
α-2-Macroglobulin	P01023	164 613	226	Secreted
Antithrombin-III	P01008	53 025	41	Secreted
Cathepsin	P07339	45 037	35	Organelles
Deoxyribonuclease-1	P24855	31 642	86	Secreted
Eukaryotic translation initiation factor 6	P56537	27 095	35	Cytoplasm
Fibrinogen β chain	P02675	56 577	36	Secreted
Fibrinogen γ chain	P02679	52 106	31	Secreted
Ganglioside GM2 activator	P17900	21 281	51	Organelles
Haptoglobin	P00738	45 861	34	Secreted
Heat shock-related 70 kDa protein 2	P54652	70 263	56	Other/unknown
Hemopexin	P02790	52 385	24	Secreted
Integrator complex subunit 4-like protein 1	Q96LV5	49 382	24	Other/unknown
Leucine-rich α-2-glycoprotein	P02750	38 382	72	Secreted
Multimerin-2	Q9H8L6	105 028	38	Secreted
Protein archease	Q8IWT0	19 535	35	Other/unknown
Ras-related protein Rab-5A	P20339	23 872	23	Plasmamembrane
Retinoid-inducible serine carboxypeptidase	Q9HB40	51 083	48	Secreted
Serum amyloid P-component	P02743	25 485	37	Secreted
Transmembrane protein 44	Q2T9K0	53 061	21	Plasmamembrane

sharpening of others (Fig. S3, Tables S3 and S4 in ESI†). About 44% of total identified proteins (147/333) are present only in CTRL, while about 22% are detected only in RCC UE (72/333), suggesting the occurrence of a differential protein content in the two groups (Tables 2 and 3). About 75% of identified proteins is present also in Exocarta – an updated database reporting all the identified exosome molecules – in the section regarding UE.[31] However, it is worth noting that a good percentage of identified proteins (about 25%) is not yet reported in Exocarta (Fig. 6).

The cellular localizations of the identified proteins (Fig. 7A), based on UniProtKB, an Expasy resource, indicate that the majority of them are in the plasma membrane, in vesicle-related organelles (*e.g.* cytoplasmic and membrane bound vesicles, early and late endosomes, lysosomes, secretory granules, and ER-Golgi intermediate compartment), and in the cytoskeleton. Moreover, in the RCC exosome pool, a high percentage (35%) is represented by secreted proteins, while it is reduced (only 15%) in CTRL ones.

The identified proteins were also analysed from a functional point of view (Fig. 7B), and we assessed the presence of many typical exosomal proteins, such as the component of the ESCRT machinery (TSG101), proteins involved in trafficking

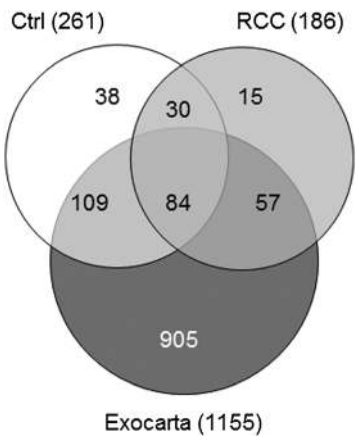

Fig. 6 Venn diagram showing the overlapping and the unique proteins identified in CTRL and RCC UE with that reported in Exocarta UE.

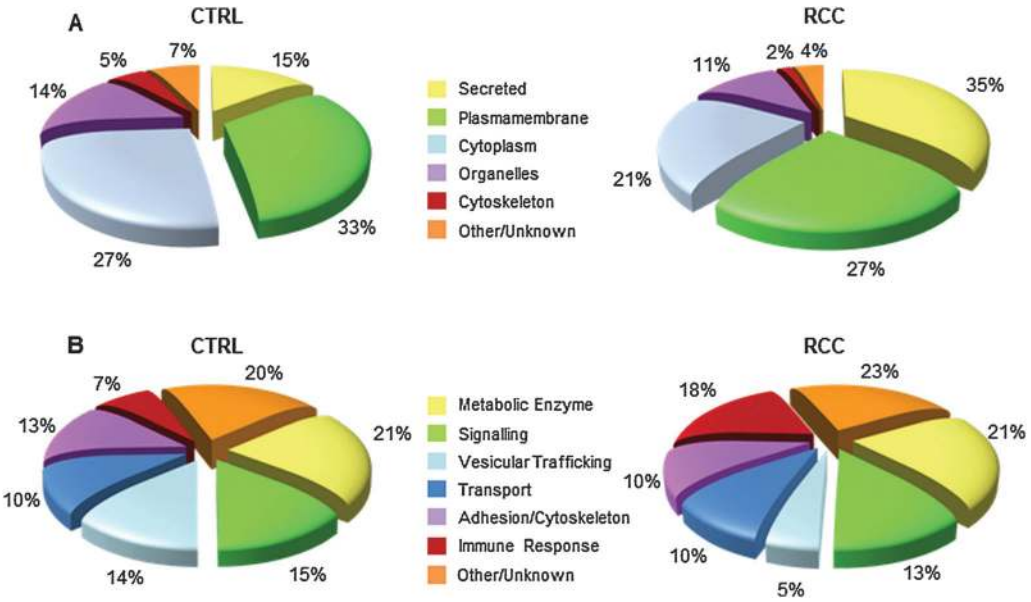

Fig. 7 Bioinformatic analysis of UE proteins. (A) Subcellular localization; (B) molecular functions.

and membrane fusion (annexins), and tetraspanins such as CD9, possibly correlated to the exosome biogenesis mechanism.[30] Moreover, many other functional classes were recognized, such as metabolic enzymes (*i.e.* triosophosphate isomerase, isocitrate dehydrogenase), proteins involved in signalling (*i.e.* Ras-related proteins), related to cellular adhesion and motility (*i.e.* ezrin, syntenin 1), communication (G-proteins), and transport (*i.e.* chloride intracellular channel protein 1 CLIC1). The presence of these proteins highlights the UE cellular origin. A consistent difference between the two pools concerns the percentage of immunity related proteins. In fact they are 18% for RCC and 7% for control exosomes. Although it must be considered that each protein is counted once in this classification, regardless of its absolute content, this result may be related to the activation of the immune system encountered in neoplastic diseases, and to one of the putative functions of exosomes, which is immune system regulation. Furthermore, many species in this group belong to the immunoglobulin family, providing a possible explanation for the above reported increase of secreted proteins in tumour exosomes.

Despite the well-known involvement of angiogenesis in RCC, only a few proteins related to this function were found in our proteomic analysis of urinary exosomes. A possible explanation for this finding is that the tumour cells may retain such strategic molecules, or release them towards the internal microenvironment;[32] on the other hand, it has to be underlined that our analytical condition did not allow for the identification of low abundant UE proteins. Moreover, the fact that urinary exosomes are not a preferred vehicle for these kinds of molecules is also suggested by their under-representation in an extensive list of UE proteins recently published.[33]

When we compared the enrichment of the biological functions on the same scale (by Ingenuity Pathway Analysis resource), the analysis showed that the profile of biological functions associated with RCC UE proteins differs considerably from CTRL ones (Fig. 8). In fact, the species related to cell death, scavenger of free radicals and cellular movement are more enriched in pathological UE, while molecular transport class is enriched in controls.

Western blot

To further validate the differential proteomic profiles of UE from RCC patients compared to controls, we examined some

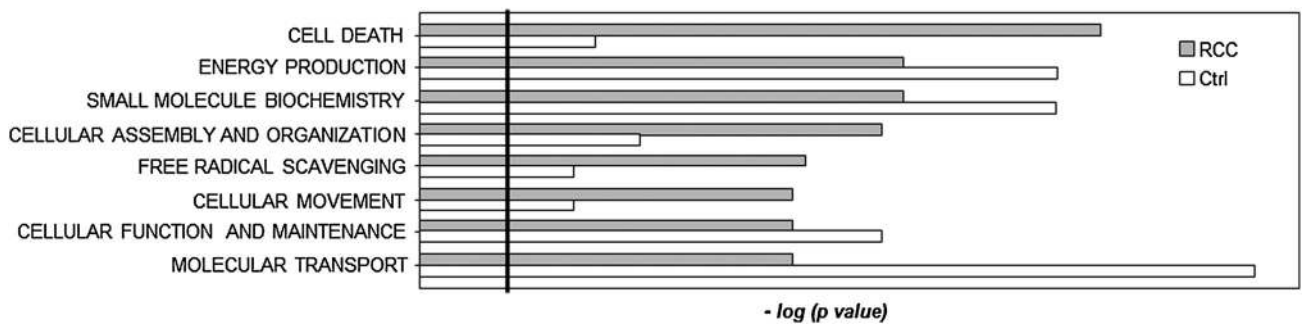

Fig. 8 Top biological functions of proteins identified in RCC and CTRL UE. The significance of the enrichment is expressed as the −log (*p* value).

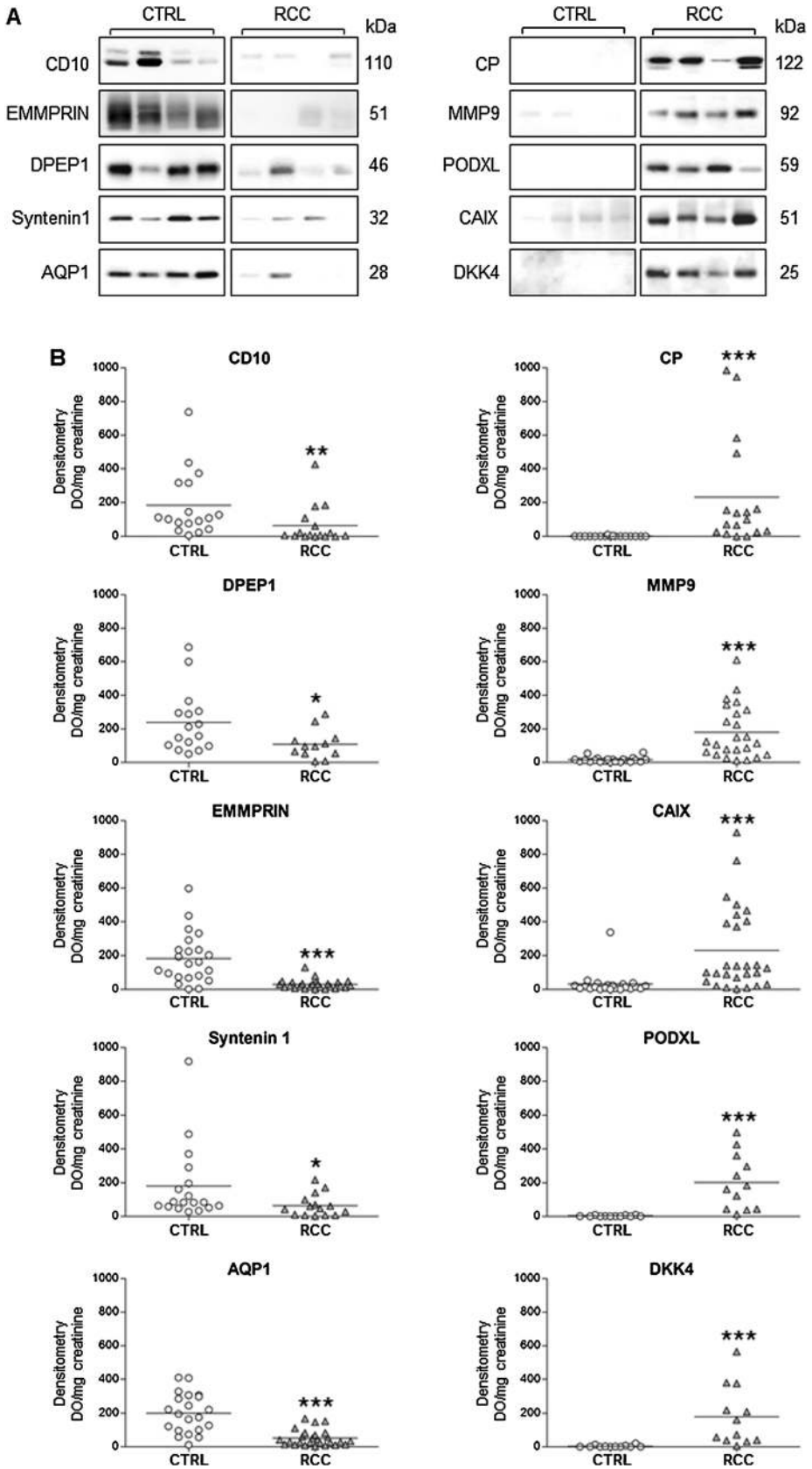

Fig. 9 Validation of differential RCC and Ctrl UE protein content by western blotting. (A) 4 representative cases are shown. (B) Densitometric quantification of bands after normalization by creatinine values. * = $p < 0.05$, ** = $p < 0.005$, *** = $p < 0.0001$.

protein levels in UE. Protein selection was based on several criteria including (1) our previous results obtained by gene and protein expression profiling on RCC tissue samples;[26,34] (2) their potential roles in contributing to RCC diagnosis, and (3) the availability of commercial antibodies. Based on the above criteria, we selected a panel of 10 proteins, and subjected their UE differential content to validation using western blot analysis (Fig. 9A). After densitometric quantification of band intensity, results were expressed as DO per mg of creatinine in Fig. 9B. Results show that Matrix metalloproteinase 9 (MMP-9), Ceruloplasmin (CP), Podocalyxin (PODXL), Dickkopf related protein 4 (DKK4) and Carbonic Anhydrase IX (CAIX) are significantly more abundant in RCC patient UE, while Aquaporin-1 (AQP1), Extracellular Matrix Metalloproteinase Inducer (EMMPRIN), Neprilysin (CD10), Dipeptidase 1 and Syntenin-1 display a significant reduced content in RCC patient's UE.

MMP9, DKK4 and EMMPRIN are involved in extracellular matrix remodeling.[35–37] Moreover, it has been reported that these three proteins are overexpressed in RCC and correlate with RCC aggressiveness and high RCC metastatic potential by promoting tumor cell migration and invasion.[26,36,38,39] Accordingly, the MMP9 and DKK4 increased content in RCC UE could be correlated to these features. This hypothesis is supported by a recent paper showing that exosomes derived from gynecologic neoplasias contain metalloproteinases that increase extracellular matrix degradation and augment tumor invasion into the stroma.[36] In contrast, EMMPRIN could be retained by tumor cells, because of its capability to induce the activation of the extracellular matrix metalloproteases such as MMP9, thus explaining its reduced content in RCC urinary exosomes, compared to control ones.

PODXL and AQP1 are typical proteins expressed by human kidney: PODXL is highly expressed in podocytes and is important for the maintenance of the cellular morphology and the anti-adhesive properties of these cells,[40] while AQP1 is a membrane water channel physiologically expressed by the proximal tubule and the loop of Henle. AQP1 (both mRNA and protein) was reported to be downregulated in RCC tissues.[41,42] Its reduction may be related to the loss of cellular specialization, a sort of ''dedifferentiation'' strategy; this could explain also its decreased content in UE. PODXL, in contrast, has recently emerged as a malignant marker in tumors arising from a variety of tissues, including also RCC.[43] Syntenin-1, in contrast to PODXL, is reported to be involved in the cellular adhesion by coupling the syndecan-2 to the cytoskeleton.[44] It is expressed, among other tissues, also in the kidney, and is a typical exosomal protein.[31]

DPEP1 is important for the physiological activity of renal cells, in particular in glutathione metabolism; for this reason it may be eliminated in urinary exosomes by tumour cells as another possible strategy to promote tumor development and progression, due to the reduction of the free radical detoxification power.[45] Neprilysin (CD10) is normally expressed by the proximal tubules and by the glomerular epithelial cells: it is a zinc-dependent metallopeptidase, which is involved in the metabolism of a number of regulatory peptides and plays an important role in turning off peptide signalling at the cell surface.[46] Loss or decrease in neprilysin expression has been reported in many types of malignancies, including renal cancer.[34,47] DPEP1 and CD10 demonstrate to have a reduced content in RCC UE, compared to control ones, possibly according to the loss of the cellular specialization, as already mentioned.

Finally, the levels of CAIX and CP are found significantly increased in RCC urinary exosomes: it has to be underlined that their promoters were reported to be activated by the transcriptional factor HIF-1α, known to be involved in RCC genesis.[48–50] In particular, gene expression profiling on renal tissue showed a marked CP mRNA overexpression in RCC patients compared to controls,[34,51] while CAIX is proven to be a powerful tissue marker for ccRCC and was recently shown to correlate with tumor size.[52] Both CP and CAIX have been detected in RCC patient serum.[52,53]

Summarizing, protein profiling and validation results indicate that the pattern of RCC UE resembles that of cancer tissue for some proteins, but it displays quite distinctive and specific features overall. As such, our data indicate that the RCC patient's UE protein profile significantly differs from that of control subjects (Fig. 10). It has to be underlined that also the RCC UE lipid composition was recently demonstrated to be differential,[54] providing further evidence for a relationship between UE composition and RCC disease.

Western blot results were then used to generate ROC curves, to predict the potential impact for use of the biomarker candidates in discriminating between the RCC group and the controls; the AUC values were determined for each protein and range between 0.73–1. In particular, CP and PODXL resulted to have AUC equal to 1, suggesting to be best at distinguishing RCC patients from the control group. The ROC curves and the AUC values of the other 8 proteins are shown in Fig. 11. Thus, these results could constitute a basis for the set-up of a multimarker strategy in UE for RCC detection. This approach would guarantee a more valid diagnostic result compared to the single markers, because less dependent upon the inter-individual differences, typical of polygenic diseases. In fact, although CP seems to have the best diagnostic performance, in AUC terms,

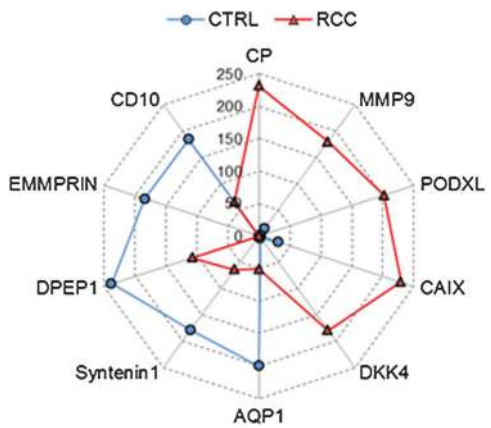

Fig. 10 Radar plot comparing the different levels of selected proteins (derived from Fig. 9A and B) in RCC and CTRL UE.

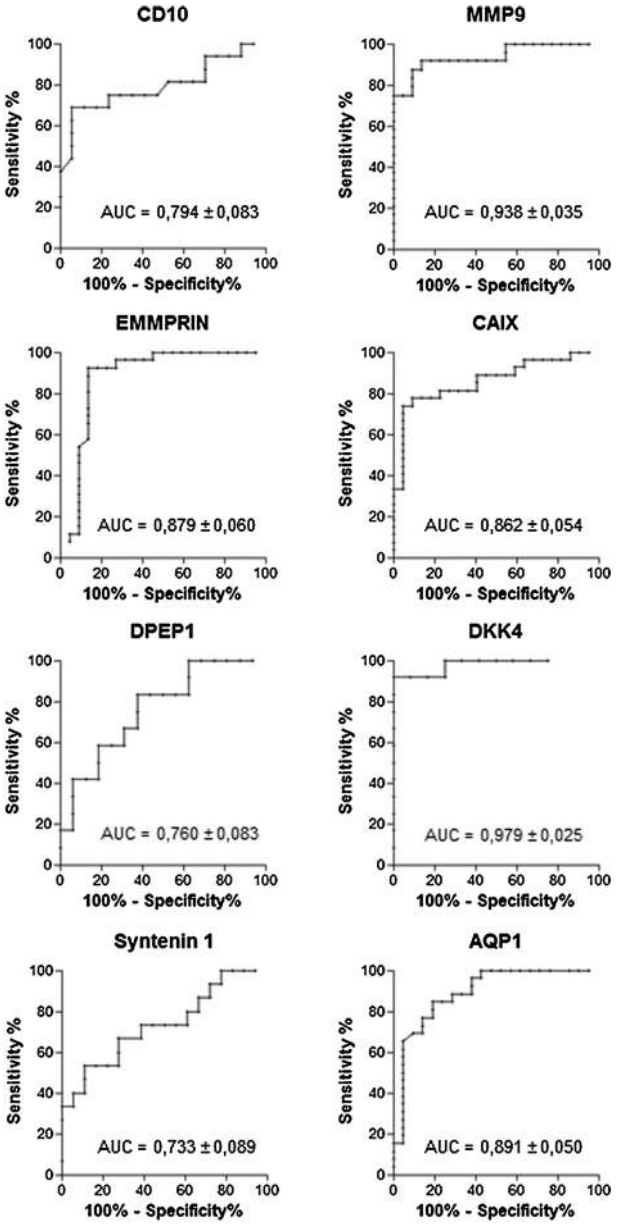

Fig. 11 ROC curves (generated by GraphPad Prism 5, GraphPad Software, Inc.) for the differentiation between CTRL and RCC through each of the 8 proteins. The AUC, sensitivity, and specificity for each protein are shown.

it has been suggested that its increase in RCC serum could be part of an acute phase response to the cancer as an unspecific marker of inflammation.[53] Moreover, it is likely that the use of multiple markers will assure a better specificity towards clear cell RCC, than the single one: the assessment of this hypothesis deserves further investigation.

Finally, in order to get a more comprehensive portrait of differential RCC protein abundance in exosomes, an appealing solution is represented by a protein microarray format along with western blot. It could give sensitive, real-time and multiplexed detection on a targeted set of specific proteins, and would allow us to validate a panel of discriminating proteins. Then the protein microarray could be easily used for diagnosis or post-surgery monitoring of RCC. We intend to evaluate this approach in a future work.

Concluding remarks

To the best of our knowledge, this is the first proteomic study performed on urinary exosomes obtained from RCC patients. Taken together, the present results show that (1) due to their biochemical and morphological characteristics, vesicles isolated by ultracentrifugation from urine samples collected from patients and controls are enriched in ''bona fide'' exosomes; (2) UE proteome represents a peculiar and readily isolated subset of the urinary proteome, and is enriched in cell-derived proteins, which may possibly be involved in the RCC pathogenesis or progression; (3) RCC UE protein content is substantially and reproducibly different from the control UE one.

In conclusion, our work suggests that exosome isolation may provide an efficient first step in RCC biomarker discovery in urine.

Acknowledgements

Grants from FIRB: Rete Nazionale per lo studio del proteoma umano (n. RBRN07BMCT) are acknowledged. We thank Dr Rosanna Falbo for skillful language revision.

References

1 B. J. Drucker, *Cancer Treat. Rev.*, 2005, **31**, 536–545.
2 E. C. Nelson, C. P. Evans and P. N. Lara Jr., *Cancer Treat. Rev.*, 2007, **33**, 299–313.
3 R. A. Craven, N. S. Vasudev and R. E. Banks, *Clin. Biochem.*, 2012, DOI: 10.1016/j.clinbiochem.2012.11.029.
4 B. I. Rini, S. C. Campbell and B. Escudier, *Lancet*, 2009, **373**, 1119–1132.
5 M. M. Vickers and D. Y. Heng, *Target. Oncol.*, 2010, **5**, 85–94.
6 M. Hernandez-Yanez, J. V. Heymach and A. J. Zurita, *Curr. Oncol. Rep.*, 2012, **14**, 221–229.
7 P. G. Moon, J. E. Lee, S. You, T. K. Kim, J. H. Cho, I. S. Kim, T. H. Kwon, C. D. Kim, S. H. Park, D. Hwang, Y. L. Kim and M. C. Baek, *Proteomics*, 2011, **11**, 2459–2475.
8 I. M. Rood, J. K. Deegens, M. L. Merchant, W. P. Tamboer, D. W. Wilkey, J. F. Wetzels and J. B. Klein, *Kidney Int.*, 2010, **78**, 810–816.
9 E. Cocucci, G. Racchetti and J. Meldolesi, *Trends Cell. Biol.*, 2009, **19**, 43–51.
10 B. Fevrier and G. Raposo, *Curr. Opin. Cell Biol.*, 2004, **16**, 415–421.
11 C. Thery, L. Zitvogel and S. Amigorena, *Nat. Rev. Immunol.*, 2002, **2**, 569–579.
12 E. J. Hoorn, T. Pisitkun, R. Zietse, P. Gross, J. Frokiaer, N. S. Wang, P. A. Gonzales, R. A. Star and M. A. Knepper, *Nephrology*, 2005, **10**, 283–290.
13 Y. Li, Y. Zhang, F. Qiu and Z. Qiu, *Electrophoresis*, 2011, **32**, 1976–1983.
14 H. Sonoda, N. Yokota-Ikeda, S. Oshikawa, Y. Kanno, K. Yoshinaga, K. Uchida, Y. Ueda, K. Kimiya, S. Uezono,

A. Ueda, K. Ito and M. Ikeda, *Am. J. Physiol.*, 2009, **297**, F1006–F1016.
15 J. Conde-Vancells and J. M. Falcon-Perez, *Methods Mol. Biol.*, 2012, **909**, 321–340.
16 N. van der Lubbe, P. M. Jansen, M. Salih, R. A. Fenton, A. H. van den Meiracker, A. H. Danser, R. Zietse and E. J. Hoorn, *Hypertension*, 2012, **60**, 741–748.
17 J. L. Welton, S. Khanna, P. J. Giles, P. Brennan, I. A. Brewis, J. Staffurth, M. D. Mason and A. Clayton, *Mol. Cell. Proteomics*, 2010, **9**, 1324–1338.
18 T. Pisitkun, M. T. Gandolfo, S. Das, M. A. Knepper and S. M. Bagnasco, *Proteomics: Clin. Appl.*, 2012, **6**, 268–278.
19 P. G. Moon, S. You, J. E. Lee, D. Hwang and M. C. Baek, *Mass Spectrom. Rev.*, 2011, **30**, 1185–1202.
20 Y. Nagashima, Y. Inayama, Y. Kato, N. Sakai, H. Kanno, I. Aoki and M. Yao, *Pathol. Int.*, 2004, **54**, 377–386.
21 H. Zhou, P. S. Yuen, T. Pisitkun, P. A. Gonzales, H. Yasuda, J. W. Dear, P. Gross, M. A. Knepper and R. A. Star, *Kidney Int.*, 2006, **69**, 1471–1476.
22 T. Pisitkun, R. F. Shen and M. A. Knepper, *Proc. Natl. Acad. Sci. U. S. A.*, 2004, **101**, 13368–13373.
23 S. Mathivanan, J. W. Lim, B. J. Tauro, H. Ji, R. L. Moritz and R. J. Simpson, *Mol. Cell. Proteomics*, 2010, **9**, 197–208.
24 M. Schroder, R. Schafer and P. Friedl, *Anal. Biochem.*, 1997, **244**, 174–176.
25 V. Aggelis, R. A. Craven, J. Peng, P. Harnden, D. A. Cairns, E. R. Maher, R. Tonge, P. J. Selby and R. E. Banks, *Proteomics*, 2009, **9**, 2118–2130.
26 F. Raimondo, L. Morosi, C. Chinello, R. Perego, C. Bianchi, G. Albo, S. Ferrero, F. Rocco, F. Magni and M. Pitto, *Mol. Biosyst.*, 2012, **8**, 1007–1016.
27 P. J. Mitchell, J. Welton, J. Staffurth, J. Court, M. D. Mason, Z. Tabi and A. Clayton, *J. Transl. Med.*, 2009, **7**, 4.
28 J. W. Dear, J. M. Street and M. A. Bailey, *Proteomics*, 2012, DOI: 10.1002/pmic.201200285.
29 D. A. Raj, I. Fiume, G. Capasso and G. Pocsfalvi, *Kidney Int.*, 2012, **81**, 1263–1272.
30 F. Raimondo, L. Morosi, C. Chinello, F. Magni and M. Pitto, *Proteomics*, 2011, **11**, 709–720.
31 S. Mathivanan, C. J. Fahner, G. E. Reid and R. J. Simpson, *Nucleic Acids Res.*, 2012, **40**, D1241–D1244.
32 J. E. Park, H. S. Tan, A. Datta, R. C. Lai, H. Zhang, W. Meng, S. K. Lim and S. K. Sze, *Mol. Cell. Proteomics*, 2010, **9**, 1085–1099.
33 Z. Wang, S. Hill, J. M. Luther, D. L. Hachey and K. L. Schey, *Proteomics*, 2012, **12**, 329–338.
34 I. Cifola, R. Spinelli, L. Beltrame, C. Peano, E. Fasoli, S. Ferrero, S. Bosari, S. Signorini, F. Rocco, R. Perego, V. Proserpio, F. Raimondo, P. Mocarelli and C. Battaglia, *Mol. Cancer*, 2008, **7**, 6.
35 J. F. Woessner Jr., *FASEB J.*, 1991, **5**, 2145–2154.
36 H. Hirata, Y. Hinoda, S. Majid, Y. Chen, M. S. Zaman, K. Ueno, K. Nakajima, Z. L. Tabatabai, N. Ishii and R. Dahiya, *Cancer*, 2011, **117**, 1649–1660.
37 E. Huet, E. E. Gabison, S. Mourah and S. Menashi, *Connect. Tissue Res.*, 2008, **49**, 175–179.
38 N. H. Cho, H. S. Shim, S. Y. Rha, S. H. Kang, S. H. Hong, Y. D. Choi, S. J. Hong and S. H. Cho, *Eur. Urol.*, 2003, **44**, 560–566.
39 Y. X. Liang, H. C. He, Z. D. Han, X. C. Bi, Q. S. Dai, Y. K. Ye, W. J. Qin, G. H. Zeng, G. Zhu, C. L. Xu and W. D. Zhong, *Cancer Invest.*, 2009, **27**, 788–793.
40 R. A. Orlando, T. Takeda, B. Zak, S. Schmieder, V. M. Benoit, T. McQuistan, H. Furthmayr and M. G. Farquhar, *J. Am. Soc. Nephrol.*, 2001, **12**, 1589–1598.
41 J. Takenawa, Y. Kaneko, M. Kishishita, H. Higashitsuji, H. Nishiyama, T. Terachi, Y. Arai, O. Yoshida, M. Fukumoto and J. Fujita, *Int. J. Cancer*, 1998, **79**, 1–7.
42 D. Ticozzi-Valerio, F. Raimondo, M. Pitto, F. Rocco, S. Bosari, R. Perego, C. Sarto, A. Di Fonzo, N. Bosso, P. Mocarelli, M. Galli-Kienle and F. Magni, *Proteomics: Clin. Appl.*, 2007, **1**, 588–597.
43 Y. H. Hsu, W. L. Lin, Y. T. Hou, Y. S. Pu, C. T. Shun, C. L. Chen, Y. Y. Wu, J. Y. Chen, T. H. Chen and T. S. Jou, *Am. J. Pathol.*, 2010, **176**, 3050–3061.
44 M. F. Baietti, Z. Zhang, E. Mortier, A. Melchior, G. Degeest, A. Geeraerts, Y. Ivarsson, F. Depoortere, C. Coomans, E. Vermeiren, P. Zimmermann and G. David, *Nat. Cell Biol.*, 2012, **14**, 677–685.
45 G. Zhang, A. Schetter, P. He, N. Funamizu, J. Gaedcke, B. M. Ghadimi, T. Ried, R. Hassan, H. G. Yfantis, D. H. Lee, C. Lacy, A. Maitra, N. Hanna, H. R. Alexander and S. P. Hussain, *PLoS One*, 2012, **7**, e31507.
46 A. J. Turner, R. E. Isaac and D. Coates, *Bioessays*, 2001, **23**, 261–269.
47 J. Conde-Vancells, E. Rodriguez-Suarez, E. Gonzalez, A. Berisa, D. Gil, N. Embade, M. Valle, Z. Luka, F. Elortza, C. Wagner, S. C. Lu, J. M. Mato and M. Falcon-Perez, *Proteomics: Clin. Appl.*, 2010, **4**, 416–425.
48 V. Medina Villaamil, G. Aparicio Gallego, I. Santamarina Cainzos, M. Valladares-Ayerbes and L. M. Anton Aparicio, *Clin. Transl. Oncol.*, 2012, **14**, 698–708.
49 C. K. Mukhopadhyay, B. Mazumder and P. L. Fox, *J. Biol. Chem.*, 2000, **275**, 21048–21054.
50 A. B. Stillebroer, P. F. Mulders, O. C. Boerman, W. J. Oyen and E. Oosterwijk, *Eur. Urol.*, 2010, **58**, 75–83.
51 A. O. Osunkoya, Q. Yin-Goen, J. H. Phan, R. A. Moffitt, T. H. Stokes, M. D. Wang and A. N. Young, *Hum. Pathol.*, 2009, **40**, 1671–1678.
52 G. X. Zhou, J. Ireland, P. Rayman, J. Finke and M. Zhou, *Urology*, 2010, **75**, 257–261.
53 M. Pejovic, V. Djordjevic, I. Ignjatovic, T. Stamenic and V. Stefanovic, *Int. Urol. Nephrol.*, 1997, **29**, 427–432.
54 P. Del Boccio, F. Raimondo, D. Pieragostino, L. Morosi, G. Cozzi, P. Sacchetta, F. Magni, M. Pitto and A. Urbani, *Electrophoresis*, 2012, **33**, 689–696.